DALTON
FULL PAPER

The interaction of 2-arsa- and 2-stiba-1,3-dionato lithium complexes with Group 8–12 metal halides

Cameron Jones,*[a] Peter C. Junk,[b] Jonathan W. Steed,[c] Ryan C. Thomas[a] and Thomas C. Williams[a]

[a] *Department of Chemistry, University of Wales, Cardiff, P.O. Box 912, Park Place, Cardiff, UK CF10 3TB*
[b] *Department of Chemistry, James Cook University, Townsville, Qld, 4811, Australia*
[c] *Department of Chemistry, King's College London, Strand, London, UK WC2R 2LS*

Received 6th June 2001, Accepted 16th August 2001
First published as an Advance Article on the web 15th October 2001

The reactivity of a range of 2-arsa- and 2-stiba-dionato lithium complexes, $[\{(solv)Li\{E[C(O)R]_2\}\}_2]$, E = As or Sb, R = alkyl or aryl, toward a variety of Group 8–12 transition metal complexes has been examined. The heterodionate ligands in the generated complexes have displayed a variety of coordination modes which in many cases have been confirmed by X-ray crystallographic studies. Modes that were encountered were η^1-As or Sb in $[(C_5Me_5)Fe(CO)_2\{As[C(O)Ph]_2\}]$, *trans*-$[PtCl(PEt_3)_2\{As[C(O)Ph]_2\}]$ and *trans*-$[PtCl(PEt_3)_2\{Sb[C(O)(C_2H_2Me_3\text{-}2,4,6)]_2\}]$; η^2-*O,O* in $[M\{As[C(O)Bu^t]_2\}_2(DME)]$ M = Fe or Co and $[RuCl_2(PPh_3)_2\{As[C(O)Bu^t]_2\}]$; η^1-*As* : η^1-*O* : η^2-*CO* in $[RuCl(PPh_3)_2\{As[C(O)Bu^t]_2\}]$ and η^1-*As* : η^2-*O,O* in $[Zn\{As[C(O)Bu^t]_2[LiCl(DME)]\}_2]$. The syntheses of a number of related complexes are reported, as is the preparation and structural characterisation of the tetraacyldiarsane, $[As\{C(O)Ph\}_2]_2$.

Introduction

The extensive development of the field of low coordination phosphorus chemistry over the last 20 years has led to the realisation that there is a close analogy between P and the valence isoelectronic CR fragment.[1] In contrast, the poorer thermal stabilities of corresponding low coordinate arsenic and antimony compounds have hindered their evolution relative to their phosphorus counterparts.[2] In our laboratories we are involved in the further development of such compounds, especially with regard to their use as ligands in organometallic synthesis. Our efforts in this area have revealed that there can be remarkable differences in the coordination chemistries of these materials that revolve around the nature of the Group 15 element involved.

One notable class of compounds we have been examining are the 2-hetero-1,3-dionato lithium complexes, $[\{(solv)Li\{E[C(O)R]_2\}\}_2]$, **1** E = As or Sb, R = alkyl or aryl.[3] The heterodionate ligands in these compounds are closely related to β-diketonates, the complexes of which are among the most widely studied systems in inorganic chemistry and have found a variety of applications in areas ranging from organic synthesis to chemical vapour deposition (CVD) processes.[4] We wished to explore the analogy between β-diketonate–transition metal complexes and their heterodionate counterparts and saw the lithium complexes, **1**, as ideal transfer reagents for the formation of the latter. Preliminary studies in this area have led to a number of novel and often unexpected results which include the preparation of **2**–**5** from the treatment of **1** with transition metal halide complexes.[5,6] It is noteworthy that several related diacyl-arsenido and -stibanido complexes, **6**, have been reported though these were synthesised by routes not involving complexes such as **1**.[7] 0.

It was the aim of this study to systematically explore the interaction of a variety of Group 8–12 transition metal halide complexes with heterodionate complexes, the expectation being that a number of interesting structural and chemical trends would emerge depending upon the Group 15 element and transition metal involved. The results of these investigations are reported herein.

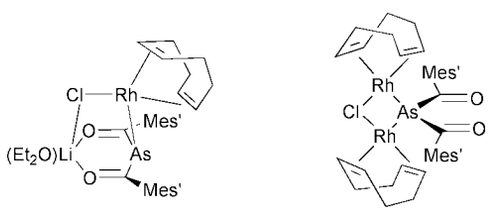

2 Mes' = $C_6H_2Pr^i_3$-2,4,6 **3**

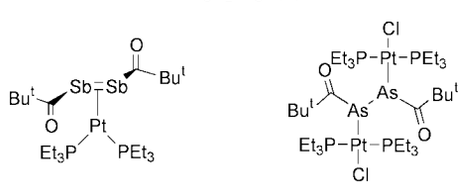

4 **5**

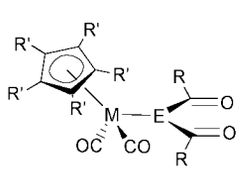

6

E = As, M = Fe, R' = H, R = Bu^t or Mesityl
E = Sb, M = Fe or Ru, R' = Me
R = Bu^t, Ph, adamantyl

Results and discussion

Group 8

The previously reported diacylarsenido–and diacylstibanido–Group 8 complexes, **6**, were prepared *via* the trimethylsilyl

elimination reactions of $[(C_5R_5)M(CO)_2E(SiMe_3)_2]$ R = H or Me, M = Fe or Ru, E = As or Sb, with two equivalents of the appropriate acyl chloride.[7] It seemed logical that similar complexes could be prepared by salt elimination reactions of lithium heterodionates with Group 8 halide complexes. Several reactions of this type were carried out and these led to the expected complexes, **7**–**9**, in moderate to good yields (Scheme 1). The

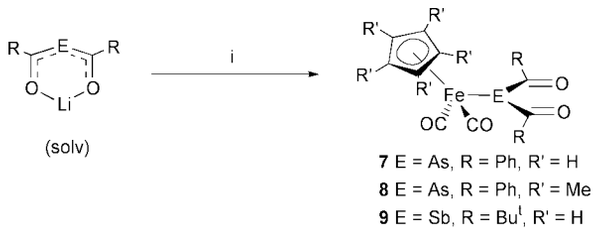

Scheme 1 *Reagents and conditions*: i, $[CpFe(CO)_2I]$ or $[Cp^*Fe(CO)_2(NCMe)][BF_4]$, DME.

spectroscopic data for these compounds are consistent with their proposed structures and similar to those seen for **6**. Most notably their IR spectra all show metal carbonyl and acyl carbonyl stretching bands in the expected regions. In addition, the ^{13}C NMR spectra of the compounds exhibit low field signals for the carbon centres associated with these groups.

As no terminal diacylarsenido Group 8 complexes have been structurally characterised an X-ray crystal structure analysis of **8** was carried out (Fig. 1). This showed it to be monomeric with the diacylarsenide ligand η^1-coordinated through a pyramidal arsenic centre. Unlike in the arsadionate precursor there appears to be no delocalisation over the ligand as both the As–C distances are normal for single bonded interactions and both C–O distances are consistent with double bonds. Although **8** contains the first structurally authenticated terminal η^1-diacylarsenide (*cf.* $\eta^1 : \eta^2$- in **2** and μ-$\eta^1 : \eta^1$- in **3**[5]) the closely related diacyl-phosphide and -stibanide complexes, $[Cp^*Ru(CO)_2P\{C(O)Bu^t\}_2]$[8] and **6**, E = Sb, M = Ru, R = Ph, R′ = Me,[7a] respectively, have been crystallographically characterised and are structurally very similar to **8**.

In order to investigate the possibility of forming the first transition metal complex in which an arsadionate ligand coordinates in an η^2-*O,O*-fashion, $FeCl_2$ was treated with two equivalents of **10** in DME (Scheme 2). This led to a moderate yield of the dark red octahedral complex, **11**. By contrast, treating $FeCl_2$ with the lithium stibadionate, **12**, afforded only an

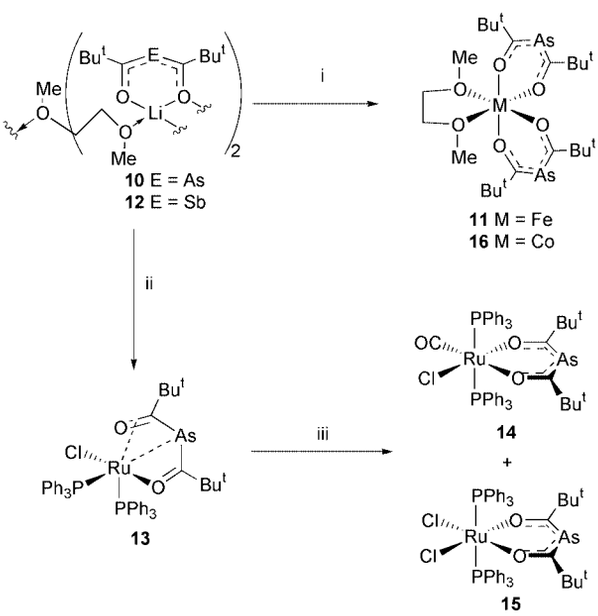

Scheme 2 *Reagents and conditions*: i, MCl_2, DME, −LiCl; ii, $[RuCl_2(PPh_3)_3]$, DME, $-PPh_3$, −LiCl; iii, CO, DME.

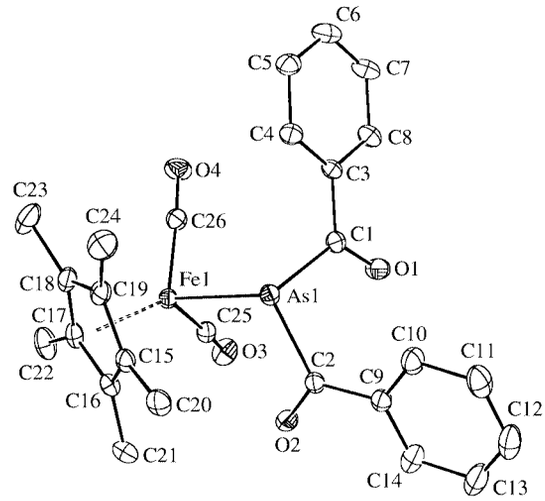

Fig. 1 Molecular structure of compound **8**. Selected bond lengths (Å) and angles (°): As(1)–C(1) 2.003(4), As(1)–C(2) 2.030(4), As(1)–Fe(1) 2.3974(7), Fe(1)–C(26) 1.746(5), Fe(1)–C(25) 1.764(5), C(1)–O(1) 1.203(5), C(2)–O(2) 1.205(5), C(25)–O(3) 1.140(5), O(4)–C(26) 1.156(5); C(1)–As(1)–C(2) 92.54(17), C(1)–As(1)–Fe(1) 109.84(11), C(2)–As(1)–Fe(1) 104.00(13), O(1)–C(1)–As(1) 121.2(3), O(2)–C(2)–As(1) 120.7(3).

intractable mixture of products. Presumably in this reaction the antimony analogue of **11** is formed but is not stable at room temperature. In addition, all attempts to form an iron(III) complex by reaction of $FeCl_3$ with three equivalents of **10** met with failure as an unidentifiable mixture of products was formed.

Compound **11** is paramagnetic with a μ_{eff} of 5.0 μ_B which corresponds to the expected 4 unpaired electrons of a high spin d^6 complex. Because of this, NMR studies on the compound gave no useful information but it was characterised by a number of other techniques. For example, its mass spectrum displayed a molecular ion peak and its infrared spectrum showed strong overlapping absorptions in the region 1500–1550 cm^{-1} which were assigned to CO stretches of the dionate ligand. In the UV/visible spectrum of the compound a broad d–d transition (ε = 19 $dm^3\ mol^{-1}\ cm^{-1}$) was observed at 758 nm and another stronger feature (ε = 380 $dm^3\ mol^{-1}\ cm^{-1}$) was noted at 515 nm. The origin of the latter peak is not known but it likely gives rise to the red-orange colour of the compound and is of an intensity normally seen for unsaturated organic ligand to metal charge transfers.[9] Cyclic voltammetric studies on **11** were not very informative but did highlight two non-reversible reductions at 0.08 V and 0.42 V *vs.* SCE using ferrocene as an internal standard. These most likely correspond to decomposition processes.

The most illuminating data on **11** came from its X-ray crystal structure analysis (Fig. 2). This proved the complex to be monomeric with a distorted octahedral geometry about the iron centre. Unlike in **8** both the arsadionate ligands coordinate the metal centre in a chelating η^2-*O,O*-fashion and are essentially planar. In addition, they appear to be largely delocalised as all the As–C bond lengths are similar (1.908 Å ave.) and lie between values normally seen for As–C single (1.96 Å)[10] and double bonds (*e.g.* 1.821(3) Å in $[CpFe(CO)_2As{=}CBu^t(OSiMe_3)]$[11]). Similarly, all the C–O bond lengths suggest delocalisation.

In an attempt to form the ruthenium analogue of **11** $[RuCl_2(PPh_3)_3]$ was treated with two equivalents of **10** in DME (Scheme 2). This led to the unexpected formation of the novel complex, **13**, in which only one of the chloride ligands of the ruthenium precursor could be substituted with an arsadionate ligand, even when the reaction was carried out at elevated temperatures. Therefore the reaction was repeated using a 1 : 1 stoichiometry and a high yield (73%) of **13** resulted. Substitution of the second chloride ligand presumably does not occur due to steric hindrance about the metal centre in the complex.

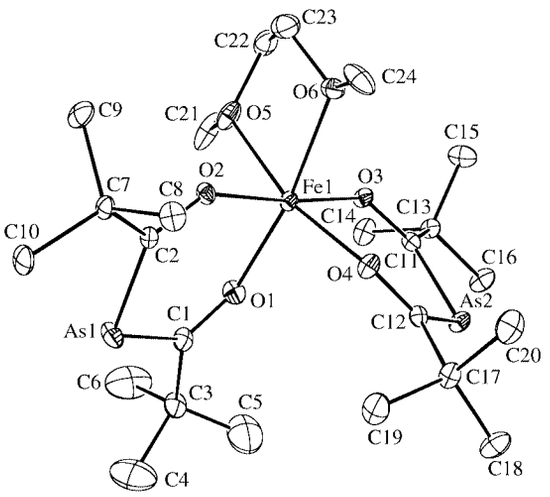

Fig. 2 Molecular structure of compound **11**. Selected bond lengths (Å) and angles (°): Fe(1)–O(1) 2.025(3), Fe(1)–O(2) 2.025(3), Fe(1)–O(4) 2.036(3), Fe(1)–O(3) 2.038(3), Fe(1)–O(5) 2.183(4), Fe(1)–O(6) 2.203(3), As(1)–C(2) 1.906(5), As(1)–C(1) 1.908(5), As(2)–C(11) 1.893(5), As(2)–C(12) 1.923(4), O(1)–C(1) 1.260(6), O(2)–C(2) 1.253(5), O(3)–C(11) 1.268(5), O(4)–C(12) 1.240(5); O(1)–Fe(1)–O(2) 89.06(13), O(3)–Fe(1)–O(4) 88.10(12), C(2)–As(1)–C(1) 100.2(2), C(11)–As(2)–C(12) 101.2(2), O(1)–C(1)–As(1) 127.2(4), O(2)–C(2)–As(1) 127.9(3), O(3)–C(11)–As(2) 127.7(3).

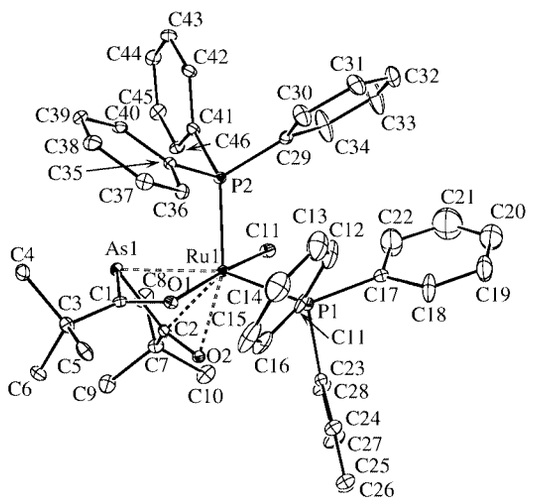

Fig. 3 Molecular structure of compound **13**. Selected bond lengths (Å) and angles (°): Ru(1)–O(1) 2.106(4), Ru(1)–O(2) 2.203(4), Ru(1)–P(2) 2.2561(16), Ru(1)–P(1) 2.3376(16), Ru(1)–Cl(1) 2.4148(17), Ru(1)–As(1) 2.5992(9), Ru(1)–C(2) 2.143(5), As(1)–C(1) 1.984(5), As(1)–C(2) 1.988(6), O(1)–C(1) 1.238(7), O(2)–C(2) 1.240(7); O(1)–Ru(1)–O(2) 76.51(15), O(1)–Ru(1)–As(1) 69.31(11), O(2)–Ru(1)–As(1) 72.20(10), C(1)–As(1)–C(2) 90.2(2), C(1)–As(1)–Ru(1) 71.75(17), C(2)–As(1)–Ru(1) 61.79(17), C(1)–O(1)–Ru(1) 106.7(3), C(2)–O(2)–Ru(1) 84.0(3), O(1)–C(1)–As(1) 112.2(4), O(2)–C(2)–As(1) 122.1(4).

The spectroscopic data for the compound are consistent with its formulation and suggest the molecule is unsymmetrical as there are two resonances in its $^{31}P\{^{1}H\}$ NMR spectrum and an inspection of its ^{1}H and ^{13}C NMR spectra confirm that the acyl fragments are chemically inequivalent. In addition, the CO stretching absorptions are at higher frequency than in delocalised systems, *e.g.* **11**, which implies that the arsadionate ligand is not fully delocalised.

To confirm this an X-ray crystal structure analysis of **13** was carried out (Fig. 3). This showed the molecule to be monomeric with a distorted octahedral geometry about the ruthenium centre. The two triphenylphosphine groups are *cis* to each other and the arsadionate ligand is facially coordinated in an unusual fashion. Firstly, the ligand does appear to be largely localised as both As–C distances are in the normal single bond length region and the C–O distances are close to those typically seen

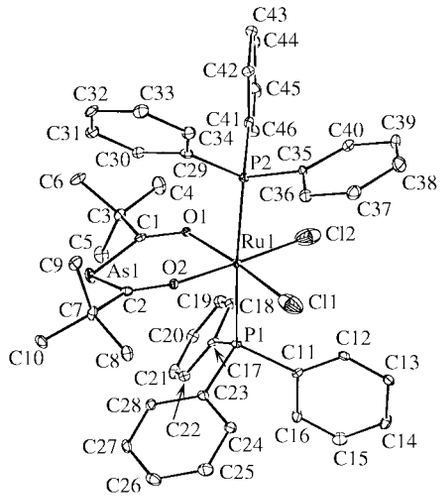

Fig. 4 Molecular structure of compound **15**. Selected bond lengths (Å) and angles (°): Ru(1)–O(2) 2.097(4), Ru(1)–O(1) 2.109(4), Ru(1)–P(1) 2.3970(18), Ru(1)–Cl(1) 2.400(4), Ru(1)–P(2) 2.4080(19), Ru(1)–Cl(2) 2.448(4), As(1)–C(2) 1.921(7), As(1)–C(1) 1.937(7), C(1)–O(1) 1.263(8), O(2)–C(2) 1.234(8); O(1)–Ru(1)–O(2) 90.94(17), Cl(1)–Ru(1)–Cl(2) 94.97(10), C(2)–As(1)–C(1) 101.9(3), O(1)–C(1)–As(1) 128.9(5), O(2)–C(2)–As(1) 128.2(5), C(1)–O(1)–Ru(1) 131.7(4), C(2)–O(2)–Ru(1) 133.9(4).

for localised double bonds. The ligand is not planar as would be expected if it was delocalised and the arsenic centre can be considered as having a heavily distorted pyramidal environment which includes a long interaction [2.5992(9) Å] to the ruthenium centre as part of its octahedral coordination (*cf.* the mean value for all crystallographically determined As–Ru bond lengths 2.44 Å[12]). The length of this bond and the distorted nature of the geometry about As(1) indicates that the ligand is strained and because it is largely localised it can be thought of as a diacylarsenide. In addition, both oxygen centres take up coordination sites at the ruthenium centre. The first of these, O(1), presumably coordinates through a lone pair [C(1)–O(1)–Ru(1) 106.7(3)°] whilst the carbonyl group containing the other, O(2), seems to be η^2-coordinated to Ru(1) [C(2)–O(2)–Ru(1) 84.0(3)°, Ru(1)–C(2) 2.143(5) Å, Ru(1)–O(2) 2.203(4) Å]. Although the Ru(1)–C(2) distance is long it does lie within the normal distance for carbonyl groups η^2-coordinated to ruthenium.[12]

Considering the weakness of the As–Ru bond in **13** it was thought that if a 2-electron donor was added to this complex the As centre might be displaced from the ruthenium centre and a more symmetrical arsadionate complex could be formed. To this end CO was passed through a red DME solution of **13** which effected a colour change to yellow and subsequent precipitation of **14** as a microcrystalline solid (Scheme 2). A preliminary X-ray structure of **14** suggested its gross molecular framework but the data were too weak for a refinement of the structure to be completed. Despite this, all the spectroscopic evidence points toward the proposed structure. The $^{31}P\{^{1}H\}$ NMR spectrum of **14** exhibits a singlet, there is a strong absorption at 1950 cm^{-1} corresponding to the CO stretch of the carbon monoxide ligand and the ^{1}H and ^{13}C NMR spectra highlight a chemical inequivalence between the two Bu^{t}CO fragments of the arsadionate ligand.

It should be noted that in the preparation of **14** several larger orange crystals were formed in addition to the bulk yellow microcrystalline material. There was not enough of this material for a full spectroscopic characterisation so its crystal structure was obtained (Fig. 4) which showed it to be the closely related Ru(III) complex, **15** (Scheme 2). It is not known how the compound was formed under the reducing conditions employed in the reaction and its preparation was not reproducible. Despite this its structure is included here for sake of

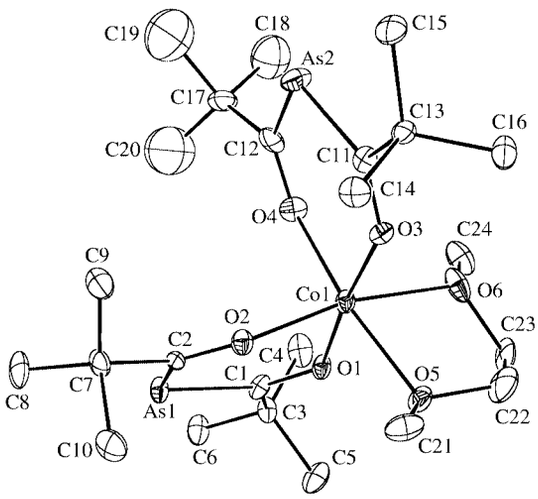

Fig. 5 Molecular structure of compound **16**. Selected bond lengths (Å) and angles (°): As(1)–C(2) 1.879(11), As(1)–C(1) 1.906(10), As(2)–C(12) 1.893(13), As(2)–C(11) 1.918(11), Co(1)–O(1) 2.025(7), Co(1)–O(2) 2.031(7), Co(1)–O(3) 1.977(7), Co(1)–O(4) 2.015(8), Co(1)–O(5) 2.179(8), Co(1)–O(6) 2.141(8), C(1)–O(1) 1.266(12), C(2)–O(2) 1.265(11), C(11)–O(3) 1.249(12), C(12)–O(4) 1.277(15); C(2)–As(1)–C(1) 100.8(4), C(12)–As(2)–C(11) 100.7(5), O(3)–Co(1)–O(4) 92.4(3), O(1)–Co(1)–O(2) 91.0(3), O(1)–C(1)–As(1) 128.6(7), O(2)–C(2)–As(1) 129.6(7), O(3)–C(11)–As(2) 127.8(8), O(4)–C(12)–As(2) 128.9(9).

comparison with **13**. It was originally thought that the structure was of **14** with the Cl and CO ligands positionally disordered. All attempts to model such a disorder met with failure and indeed the IR spectrum of a single crystal of **15** showed no CO stretch in the normal region for a coordinated carbon monoxide ligand. The ruthenium centre in the compound has a slightly distorted octahedral environment with *trans*-phosphine and *cis*-chloride ligands. The bond lengths within the planar arsadionate ligand suggest full delocalisation and unlike in **13** there is no interaction of the As centre with Ru(1).

Group 9

The only known examples of stiba- or arsa-dionate complexes of Group 9 metals are the novel rhodium complexes, **2** and **3**, recently reported by us.[5] We wished to extend this work to the formation of cobalt complexes, in particular those in which the ligand bonds in an η^2-*O,O*-mode as such simple complexes could make suitable CVD precursors. Accordingly, $CoCl_2$ was treated with two equivalents of **10** in DME to afford a moderate yield of the red-orange Co(II) complex, **16**, (Scheme 2). As was the case with the iron complex, **11**, all attempts to form the stibadionate analogue of **16** led to intractable mixtures of products, presumably due to the thermal instability of that complex. Compound **16** was revealed to be high spin (μ_{eff} 4.2 μ_B) and so solution NMR studies did not provide any useful information. However, its APCI mass spectrum exhibited a molecular ion peak. A peak was observed in its visible spectrum at a similar position and of a similar intensity (510 nm, $\varepsilon = 225$ $dm^3\ mol^{-1}\ cm^{-1}$) to that seen for **11**. Again, the origin of this peak is not known but may arise from a LMCT process. A weaker d–d transition would be expected in the general region of this peak but is probably masked by the stronger absorption. The other expected spin allowed d–d transition was not observed as it most likely exists in the near-IR region as with most octahedral Co(II) complexes. Cyclic voltammetric studies were carried out on **16** under a range of conditions but gave no useful information.

The X-ray crystal structure of **16** (Fig. 5) showed the compound to be monomeric and isomorphous to its iron analogue, **11**. As in that case the metal centre has a distorted octahedral coordination environment which includes two chelating arsadionate ligands and one DME molecule. The As–C and C–O bond lengths are close to those in **11** and strongly suggest the planar arsadionate ligands are largely delocalised. This contrasts to the situation in the rhodium complexes, **2** and **3**, which possess related localised ligands.

Group 10

In a preliminary study we have shown that the treatment of *cis*-$[PtCl_2(PEt_3)_2]$ with **10** or **12** led to the Pt(0) distibene and the Pt(II) diarsenide–dione complexes, **4** and **5**, respectively, both *via* loss of the α-diketone, $\{Bu^tC(O)\}_2$.[6] By contrast, reaction of **12** with $[MCl_2(PEt_3)_2]$, M = Ni or Pd afforded the acyl metal complexes, *trans*-$[MCl\{C(O)Bu^t\}(PEt_3)_2]$ with a concomitant deposition of an antimony mirror.[6] Therefore it was apparent that the heterodionate ligands in **10** and **12** are unstable toward E–C, E = As or Sb, bond cleavage upon coordination to Group 10 metal fragments. As a result, the possibility of altering the alkyl substituents on these ligands to form more stable complexes was examined with mixed results.

Firstly, the reaction of the phenyl substituted lithium–arsadionate, **17**, with $NiBr_2 \cdot 2DME$ did not lead to the expected arsadionate–nickel complex but instead to decomposition and deposition of insoluble arsenic containing materials. More success was had when *cis*-$[PtCl_2(PEt_3)_2]$ was treated with two equivalents of either **17** or **18** which surprisingly gave the *trans*-complexes, **19** and **20**. These were found to be stable to chloride substitution by the second equivalent of lithium heterodionate which remained in solution (Scheme 3). These compounds presumably form *via* an associative mechanism involving five-coordinate intermediates, $[PtCl_2(PEt_3)_2\{\eta^1\text{-}E[C(O)R]_2\}]$, which undergo isomerisation upon displacement of one chloride ligand. It is interesting that both **19** and **20** are stable to E–C bond cleavage when **4** and **5** are formed by such a process in very similar reactions. It can not be certain why changing the heterodionate substituents has such a great effect in these reactions but it is likely a combination of steric and electronic factors.

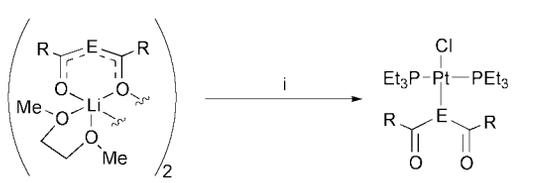

17 E = As, R = Ph
18 E = Sb, R = mesityl

19 E = As, R = Ph
20 E = Sb, R = mesityl

Scheme 3 *Reagents and conditions*: i, *cis*-$[PtCl_2(PEt_3)_2]$, DME, −LiCl.

The spectroscopic data for **19** and **20** are compatible with their proposed structures in that both show single phosphine resonances in their $^{31}P\{^1H\}$ NMR spectra. In addition, each resonance possesses platinum satellites with large $^1J_{PtP}$ couplings (**19** 3081, **20** 3296 Hz), as would be expected for chemically equivalent phosphines *trans* to each other in square planar platinum complexes. The IR spectra of both complexes display strong absorptions in the normal region for localised carbonyl groups and their ^1H NMR and mass spectra suggest only one heterodionate ligand is present in each compound.

The molecular structures of **19** and **20** are depicted in Fig. 6 and 7 respectively. Both Pt(II) compounds are monomeric and are structurally similar. Each platinum centre has a slightly distorted square planar coordination environment with *trans*-phosphine ligands and an η^1-ligated heterodionate ligand *trans* to a chloride. The E–C and C–O bond lengths in each non-planar heterodionate ligand are normal for localised single and double bonded interactions respectively. In addition, the antimony and arsenic centres have distorted pyramidal geometries and therefore each has a stereochemically active lone pair. As a consequence of this, the ligands are best thought of as diacyl pnictides (*cf.* **8**) rather than heterodionates.

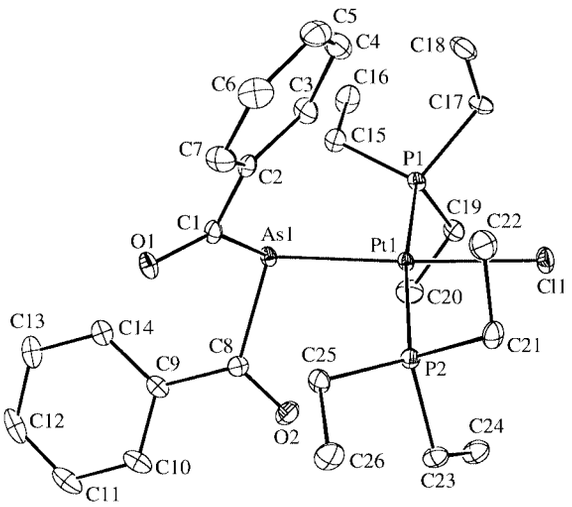

Fig. 6 Molecular structure of compound **19**. Selected bond lengths (Å) and angles (°): Cl(1)–Pt(1) 2.3989(13), As(1)–C(1) 2.006(5), As(1)–C(8) 2.012(5), As(1)–Pt(1) 2.4032(6), Pt(1)–P(1) 2.3212(13), Pt(1)–P(2) 2.3228(13), C(1)–O(1) 1.220(6), C(8)–O(2) 1.210(6); C(1)–As(1)–C(8) 99.9(2), C(1)–As(1)–Pt(1) 110.08(15), C(8)–As(1)–Pt(1) 104.09(15), Cl(1)–Pt(1)–As(1) 175.36(3), O(1)–C(1)–As(1) 120.0(4), O(2)–C(8)–As(1) 118.8(4).

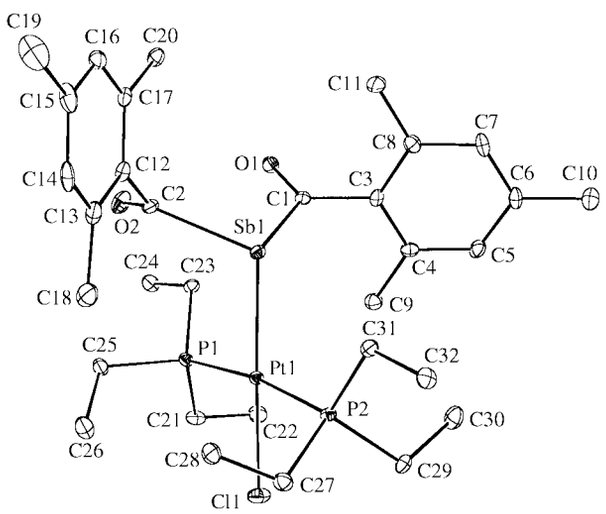

Fig. 7 Molecular structure of compound **20**. Selected bond lengths (Å) and angles (°): Pt(1)–P(1) 2.3330(14), Pt(1)–P(2) 2.3418(13), Pt(1)–Cl(1) 2.4101(13), Pt(1)–Sb(1) 2.6042(4), Sb(1)–C(1) 2.257(5), Sb(1)–C(2) 2.295(5), C(1)–O(1) 1.227(6), C(2)–O(2) 1.210(6); Cl(1)–Pt(1)–Sb(1) 173.92(3), C(1)–Sb(1)–C(2) 96.46(18), C(1)–Sb(1)–Pt(1) 104.83(13), C(2)–Sb(1)–Pt(1) 109.99(14), O(1)–C(1)–Sb(1) 123.1(4), O(2)–C(2)–Sb(1) 126.6(4).

Groups 11 and 12

There had been no reports of arsa- or stiba-dionate complexes of Group 11 or 12 metals prior to this study. We set about to reverse this situation as related β-diketonate complexes, especially of Group 11, have found application as volatile CVD precursors.[4] Consequently, it was thought that their hetero-substituted analogues might be of a similar utility if they could be prepared. Unfortunately, this did not prove to be the case as the reaction of **10** with either Cu(I) or Ag(I) salts always led to oxidative coupling reactions involving the deposition of the metal involved and the formation of the known tetraacyldiarsane, **21**[13] (Scheme 4). Similarly, the reaction of cadmium and mercury(II) halides with two equivalents of **10** gave intractable mixtures of products.

This was not the case in the reaction of **10** with $ZnCl_2$ which unexpectedly afforded the novel complex, **22**, in a moderate yield (Scheme 4). This compound can be considered as an intermediate in the intended salt elimination reaction which

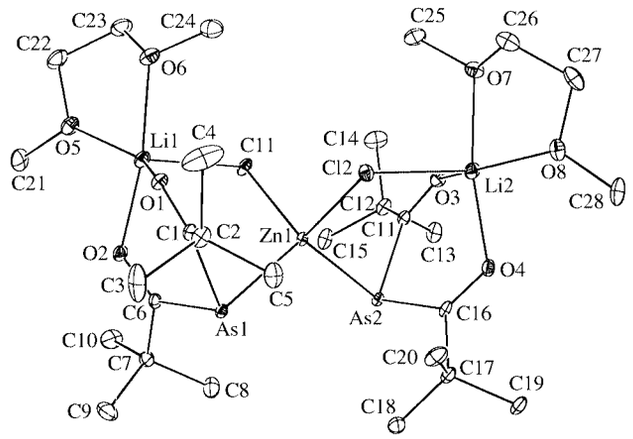

Fig. 8 Molecular structure of compound **22**. Selected bond lengths (Å) and angles (°): Zn(1)–Cl(1) 2.2939(15), Zn(1)–Cl(2) 2.2957(13), Zn(1)–As(1) 2.4933(10), Zn(1)–As(2) 2.5198(15), As(1)–C(6) 1.983(4), As(1)–C(1) 1.988(4), As(2)–C(16) 1.970(4), As(2)–C(11) 1.984(4), Cl(1)–Li(1) 2.471(7), Cl(2)–Li(2) 2.497(7), C(1)–O(1) 1.220(5), C(6)–O(2) 1.225(5), C(11)–O(3) 1.213(5), C(16)–O(4) 1.227(5); Cl(1)–Zn(1)–Cl(2) 105.54(5), Cl(1)–Zn(1)–As(1) 108.78(4), Cl(2)–Zn(1)–As(1) 109.62(4), Cl(1)–Zn(1)–As(2) 110.03(5), Cl(2)–Zn(1)–As(2) 107.98(5), As(1)–Zn(1)–As(2) 114.51(4), C(6)–As(1)–C(1) 97.57(16), C(6)–As(1)–Zn(1) 92.61(11), C(1)–As(1)–Zn(1) 91.27(11), C(16)–As(2)–C(11) 98.76(16), C(16)–As(2)–Zn(1) 91.50(12), C(11)–As(2)–Zn(1) 88.56(11), Zn(1)–Cl(1)–Li(1) 98.45(16), Zn(1)–Cl(2)–Li(2) 100.83(16).

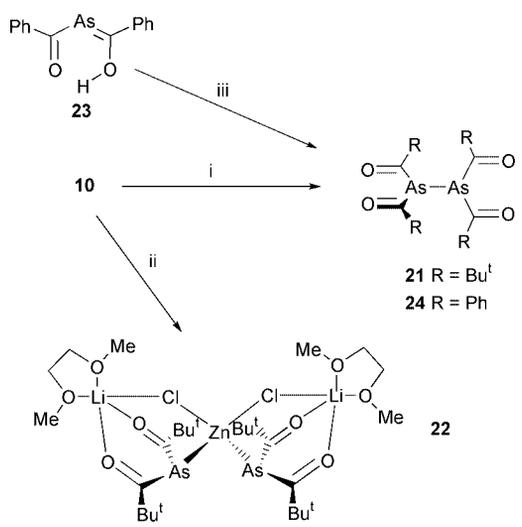

Scheme 4 *Reagents and conditions*: i, CuCl or AgCl, $-Cu_{(s)}$ or $Ag_{(s)}$; ii, $ZnCl_2$, DME; iii, $[Hg\{N(SiMe_3)_2\}_2]$, DME, $-HN(SiMe_3)_2$, $-Hg_{(l)}$.

was proposed to yield a chelated arsadionate–zinc complex. Despite this, stirring solutions of **22** for extended periods at room temperature led to no further reaction and at elevated temperatures decomposition occurred. A parallel can be drawn between **22** and **2**, the latter of which was found to be a trapped intermediate in a salt elimination reaction that yielded **3**.

The spectroscopic data for **22** are all consistent with its proposed structure which was confirmed by an X-ray crystal structure analysis. Its molecular structure (Fig. 8) can be best described as containing a tetrahedrally coordinated zinc centre which is η^1-ligated by two largely localised diacylarsenide ligands, each of which also chelates a LiCl(DME) fragment through its oxygen lone pairs. These fragments themselves coordinate the zinc centre through chloride lone pairs. The distance of these interactions is very close to the mean Zn–Cl bond length, 2.270 Å.[12] Each arsenic centre has a distorted pyramidal geometry and both Zn–As distances represent the shortest yet reported.

Considering that reactions of **10** with Group 12 dihalides did not give the expected arsadionate complexes another strategy was employed. This involved the reaction of two equivalents of

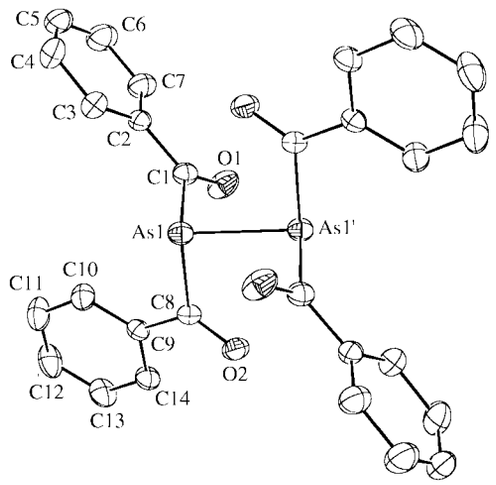

Fig. 9 Molecular structure of compound **24**. Selected bond lengths (Å) and angles (°): As(1)–C(8) 2.017(3), As(1)–C(1) 2.051(3), As(1)–As(1)′ 2.4254(6), C(1)–O(1) 1.198(4), C(8)–O(2) 1.212(3); C(8)–As(1)–C(1) 93.75(12), C(8)–As(1)–As(1)′ 90.13(9), C(1)–As(1)–As(1)′ 91.88(9), O(1)–C(1)–As(1) 119.4(2), O(2)–C(8)–As(1) 118.6(2).

the 2-arsa-1,3-dione, **23**, with Group 12 amide complexes, $[M\{N(SiMe_3)_2\}_2]$, M = Zn, Cd or Hg. It was hoped that this would lead to amine elimination and formation of arsadionate complexes. However, when M = Zn or Cd a reaction occurred but only a complex mixture of products resulted. By contrast, the reaction with $[Hg\{N(SiMe_3)_2\}_2]$ was cleaner and the tetraacyldiarsane, **24**, was isolated in moderate yield (Scheme 4). It is likely that this compound arises from an initially formed intermediate, $[Hg\{As[C(O)Ph]_2\}_2]$, which is unstable at room temperature and decomposes to give **24** *via* an oxidative coupling reaction involving a simultaneous elimination of elemental mercury.

The spectroscopic data for **24** are unexceptional and are compatible with the structure depicted in Scheme 4. This was verified by an X-ray crystal structure analysis which shows the molecule (Fig. 9) to be dimeric with two pyramidal arsenic centres generated by a crystallographic centre of inversion. Both the As–As and As–C bond lengths are typical for single bonds and all the C–O distances are in the double bond range. The structure is similar to that of the only other crystallographically characterised tetraacyldiarsane, **21**.[13]

Conclusions

In summary, we have described the interaction of a range of arsa- and stiba-dionatolithium complexes with a variety of Group 8–12 halide complexes. This work builds upon preliminary results and highlights the versatile nature of the heterodionate ligand system which has exhibited a diverse array of coordination modes. Although these ligands can behave similarly to their β-diketonate counterparts they normally do not. It can be expected that they will form a similar array of novel complexes with both early transition and main group metals. We are currently investigating this area and will report on it in a forthcoming series of publications. In addition we are exploring the utility of complexes such as **11** and **16** as potential CVD precursors to either the metal involved or binary metal–pnictide materials. The results of this study will be reported in due course.

Experimental

General remarks

All manipulations were carried out using standard Schlenk and glove box techniques under an atmosphere of high purity argon or dinitrogen. The solvents diethyl ether, hexane, toluene and DME were distilled over either potassium or Na/K alloy then freeze/thaw degassed prior to use. ^{1}H, ^{13}C and ^{31}P NMR spectra were recorded on Bruker AMX360, WM250, DPX400 or JEOL Eclipse 300 spectrometers in C_6D_6 and were referenced to the residual ^{1}H resonances of the solvent used (^{1}H NMR) or to external 85% H_3PO_4, 0.0 ppm (^{31}P NMR). Mass spectra were recorded using a VG Fisons Platform II instrument under EI or APCI conditions. UV/visible spectra were recorded on a Perkin-Elmer Lambda 20 machine. Magnetic susceptibilities were determined using the Evans method.[14] Electrochemical studies were carried out on Autolab PGStat 12 instrument using an 0.1 M dichloromethane solution of NBu_4PF_6 as a supporting electrolyte and ferrocene as an internal standard. Melting points were determined in sealed glass capillaries under argon, and are uncorrected. Elemental analyses were carried out at the Warwick Analytical Service. The starting materials **10**,[3] **12**,[3] **17**,[15] **18**[15] and **23**[15] were prepared by literature procedures. All other reagents were used as received.

Syntheses

$[(C_5H_5)Fe(CO)_2\{As[C(Ph)O]_2\}]$ 7. A solution of **17** (0.390 g, 1.02 mmol) in DME (40 ml) was added dropwise to a solution of $[CpFe(CO)_2I]$ (0.309 g, 1.02 mmol) in DME (30 ml) at −78 °C. The resulting dark red/brown solution was allowed to warm to room temperature and stirred for 24 h. Volatiles were removed *in vacuo* leaving a dark brown residue which was extracted with diethyl ether (3 × 30 ml), filtered and the filtrate placed at −30 °C yielding **7** as red crystals (yield 0.29 g, 63%), mp 80 °C (decomp.); NMR: ^{1}H (400 MHz, C_6D_6), δ 4.60 (5H, s, C_5H_5), 7.32–7.91 (10H, m, ArH); ^{13}C (100.6 MHz, C_6D_6), δ 85.2 (C_5H_5), 129.2 (*m*-Ar), 130.3 (*o*-Ar), 133.5 (*p*-Ar), 142.3 (quat. Ar), 214.3 (FeCO), 225.6 (AsC); IR (Nujol, ν/cm^{-1}) FeCO 1997 s, 1962 s, AsCO 1661 m, 1623 s; MS APCI: *m*/*z* 462 (M^+, 100%).

$[(C_5Me_5)Fe(CO)_2\{As[C(Ph)O]_2\}]$ 8. A solution of **17** (0.366 g, 0.96 mmol) in DME (40 ml) was added dropwise to a solution of $[Cp^*Fe(CO)_2(NCMe)][BF_4]$ (0.354 g, 0.96 mmol) in DME (30 ml) at −78 °C. The resulting dark red/brown solution was allowed to warm to room temperature and stirred for 24 h. Volatiles were removed *in vacuo* leaving a dark brown residue which was extracted with diethyl ether (3 × 30 ml), filtered and the filtrate placed at −30 °C yielding **8** as red/orange crystals (yield 0.23 g, 54%), mp 124 °C (decomp.); NMR: ^{1}H (400 MHz, C_6D_6), δ 1.56 (15H, s, C_5Me_5), 6.83–8.48 (10H, m, ArH); ^{13}C (100.6 MHz, C_6D_6), δ 11.0 (CH_3), 97.1 (C_5Me_5) 130.1 (*m*-Ar), 132.2 (*o*-Ar), 134.1 (*p*-Ar), 144.2 (quat. Ar), 217.7 (FeCO), 225.9 (AsC); IR (Nujol, ν/cm^{-1}) FeCO 1999 s, 1941 s, AsCO 1668 m, 1627 s; MS APCI: *m*/*z* 533 (MH^+, 100%).

$[(C_5H_5)Fe(CO)_2\{Sb[C(Bu^t)O]_2\}]$ 9. A solution of **12** (0.433 g, 1.26 mmol) in DME (40 ml) was added dropwise to a solution of $[CpFe(CO)_2I]$ (0.382 g, 1.26 mmol) in DME (30 ml) at −78 °C. The resulting deep red solution was allowed to warm to room temperature and stirred for 24 h. Volatiles were removed *in vacuo* leaving a dark red residue which was extracted with diethyl ether (3 × 30ml), filtered and the filtrate placed at −30 °C yielding **9** as red needles (yield 0.18 g, 30%), mp 80 °C (decomp.); NMR: ^{1}H (400 MHz, C_6D_6), δ 1.10 (18H, s, Bu^t), 4.28 (5H, s, CpH); ^{13}C (100.6 MHz, C_6D_6), δ 26.4 (C(CH_3)), 33.5 ($C(CH_3)$), 84.1 (C_5H_5), 214.0 (FeCO), 237.9 (SbC); IR (Nujol, ν/cm^{-1}) FeCO 1998 s, 1957 s, AsCO 1672 m, 1625 s; MS APCI: *m*/*z* 412 ($M^+ - Bu^t$, 100%); calc. for $C_{17}H_{23}O_4FeSb$: C 43.5, H 4.9; found: C 42.0, H 4.8%.

$[Fe\{As[C(Bu^t)O]_2\}_2(DME)]$ 11. A solution of **10** (0.514 g, 1.73 mmol) in DME (40 ml) was added dropwise to a suspension of $FeCl_2$ (0.11 g, 0.86 mmol) in DME (10 ml) at −78 °C. The resulting red solution was allowed to warm to room temperature and stirred for 24 h. Volatiles were removed *in vacuo* leaving a dark red residue which was extracted with hexane (3 × 30ml), filtered and the filtrate placed at −30 °C yielding **11** as red blocks (yield 0.20 g, 35%), mp 115 °C

(decomp.); IR (Nujol, ν/cm^{-1}) AsCO 1545 s, 1530 s; MS APCI: *m*/*z* 245 ($O_2C_2Bu^t_2As$, 45%), 169 ($O_2C_2Bu^t_2$, 100%), 85 ($COBu^t$, 56%); μ_{eff} = 5.0 μ_B; UV/vis/nm (hexane) 758 (ε 19), 515 (ε 380 dm^3 mol^{-1} cm^{-1}); calc. for $C_{24}H_{46}O_6As_2Fe$: C 45.3, H 7.24; found: C 44.93, H 7.21%.

[Ru{As[C(O)Bu^t]$_2$}Cl(PPh$_3$)$_2$] 13. A solution of **10** (0.423 g, 1.42 mmol) in DME (40 ml) was added dropwise to a solution of [$RuCl_2(PPh_3)_3$] (1.366 g, 1.42 mmol) in DME (30 ml) at −78 °C. The resulting brown suspension was allowed to warm to room temperature and stirred for 24 h after which it had turned deep red. Volatiles were removed *in vacuo* leaving a dark red residue which was washed with hexane (60 ml) and extracted with diethyl ether (3 × 30 ml), filtered and the filtrate placed at −30 °C yielding **13** as dark red needles (yield 0.94 g, 73%), mp 138 °C (decomp.); NMR: ^{1}H (300 MHz, C_6D_6), δ 0.60 (9H, s, Bu^t), 1.61 (9H, s, Bu^t), 6.80–8.21 (30H, m, ArH); ^{13}C (100.6 MHz, C_6D_6), δ 23.8 (C(CH_3)), 26.7 (C(CH_3)), 48.2 (C(CH$_3$)), 49.0 (C(CH$_3$)), 126.1–137.2 (Ph), 250.0, 256.1 (AsC); ^{31}P{^{1}H} (36.3 MHz, C_6D_6) δ 62.5, 38.2 (br s, PPh$_3$); IR (Nujol, ν/cm^{-1}) AsCO 1637 s, 1585 m; MS APCI: *m*/*z* 870 (M$^+$ − Cl, 100%); calc. for $C_{46}H_{48}O_2P_2AsRuCl$: C 61.0, H 5.3; found: C 61.30, H 5.95%.

[Ru{As[C(O)Bu^t]$_2$}Cl(CO)(PPh$_3$)$_2$] 14. Compound **13** (0.62 g, 6.85 mmol) was dissolved in DME (30 ml) and dry CO gas passed through the deep red solution for 30 min. During this time the solution changed to a yellow colour and a yellow microcrystalline material deposited from solution. This was recrystallised from DME (20 ml) to give small yellow crystals of **14** (yield 0.51 g, 79%), mp 175 °C (decomp.); NMR: ^{1}H (300 MHz, C_6D_6), δ 0.58 (9H, s, Bu^t), 0.92 (9H, s, Bu^t), 6.80–8.19 (30H, m, ArH); ^{13}C (100.6 MHz, C_6D_6), δ 24.9 (C(CH_3)), 27.8 (C(CH_3)), 49.0 (C(CH$_3$)), 50.0 (C(CH$_3$)), 126.1–136.4 (Ph), 257.0, 264.2 (AsC), RuCO not observed due to low solubility of compound; ^{31}P{^{1}H} (36.3 MHz, C_6D_6) δ 32.0 (PPh$_3$); IR (Nujol, ν/cm^{-1}) RuCO 1951 vs, AsCO 1521 s; MS APCI: *m*/*z* 898 (M$^+$ − Cl, 35%), 636 (M$^+$ − Cl − PPh$_3$, 100%).

[Co{As[C(Bu^t)O]$_2$}$_2$(DME)] 16. A solution of **10** (0.30 g, 1.01 mmol) in DME (20 ml) was added dropwise to a suspension of $CoCl_2$ (0.06 g, 0.51 mmol) in DME (10 ml) at −78 °C. The resulting light green solution was allowed to warm to room temperature and stirred for 24 h after which time it had turned dark red. Volatiles were removed *in vacuo* leaving a dark red residue which was extracted with hexane (3 × 30 ml), filtered and the filtrate placed at −30 °C yielding **16** as red blocks (yield 0.13 g, 40%) mp 102 °C (decomp.); IR (Nujol, ν/cm^{-1}) AsCO 1548 s, 1537 m; MS APCI: *m*/*z* 640 (MH$^+$, 32%), 57 (Bu^{t+}, 100%); μ_{eff} = 4.2 μ_B; UV/vis/nm (hexane) 510 (ε 225 dm^3 mol^{-1} cm^{-1}); calc. for $C_{24}H_{46}O_6As_2Co$: C 45.1, H 7.2; found: C 44.18, H 7.15%.

***trans*-[PtCl(PEt$_3$)$_2${As[C(O)Ph]$_2$}] 19.** A solution of **17** (0.53 g, 1.42 mmol) in DME (10 ml) was added dropwise to a suspension of *cis*-[$PtCl_2(PEt_3)_2$] (0.36 g, 0.7 mmol) in DME (10 ml) at −78 °C. The resulting solution was allowed to warm to room temperature and stirred for 18 h. Volatiles were removed *in vacuo* leaving a red oily residue which was washed with hexane (40 ml) and extracted with toluene (*ca.* 7 ml), filtered and the filtrate placed at −30 °C yielding **19** as orange needles (yield 0.19 g, 36%) mp 138 °C (decomp.); NMR: ^{1}H (250 MHz, C_6D_6), δ 0.98 (dt, 18H, $^3J_{PH}$ 16, $^3J_{HH}$ 7.7, P(CH_2CH_3)$_3$), 1.99 (dq, 12H, $^2J_{PH}$ 21, $^3J_{HH}$ 7.7 Hz, P(CH_2CH_3)$_3$), 7.40–8.47 (br m, 10H, ArH); ^{13}C (100.6 MHz, C_6D_6), δ 8.38 (d, $^2J_{PC}$ 5.8, $^3J_{PtC}$ 33, P(CH_2CH_3)$_3$), 14.91 (d, $^1J_{PC}$ 24.8, $^2J_{PtC}$ 41.2 Hz, P(CH_2CH_3)$_3$), 133.5, 131.8, 130.9 (ArCH), 172.1 (AsC); ^{31}P{^{1}H} (101.2 MHz, C_6D_6) δ 10.8 (s, $^1J_{PtP}$ 3081 Hz, PEt_3); IR (Nujol, ν/cm^{-1}) AsCO 1650 s, 1606 s; MS APCI: *m*/*z* 716 (M$^+$ − Cl, 23%), 105 (PhCO, 100%).

Table 1 Crystal data for compounds **8**, **11**, **13**, **15**, **16**, **19**, **20**, **22** and **24**

	8	**11**	**13**·Et$_2$O	**15**	**16**	**19**·C$_7$H$_8$	**20**	**22**	**24**
Chemical formula	$C_{26}H_{25}AsFeO_4$	$C_{24}H_{46}As_2FeO_6$	$C_{50}H_{58}AsClO_3P_2Ru$	$C_{49}H_{55}AsCl_2O_2P_2Ru$	$C_{24}H_{46}As_2CoO_6$	$C_{33}H_{48}AsClO_2P_2Pt$	$C_{32}H_{52}ClO_2P_2PtSb$	$C_{28}H_{56}As_2Cl_2Li_2O_8Zn$	$C_{28}H_{20}As_2O_4$
M	532.23	636.30	980.34	984.76	639.38	844.11	882.97	870.72	570.28
Crystal system	Monoclinic	Monoclinic	Triclinic	Triclinic	Monoclinic	Monoclinic	Monoclinic	Triclinic	Monoclinic
Space group	$P2_1/n$	$P2_1/c$	$P\bar{1}$	$P\bar{1}$	$P2_1/c$	$P2_1/c$	$P2_1/n$	$P\bar{1}$	$P2_1/c$
a/Å	11.0904(10)	10.971(2)	10.660(3)	10.279(2)	10.994(5)	15.4700(10)	18.6340(10)	10.166(4)	10.8988(10)
b/Å	15.1249(9)	15.347(3)	10.809(3)	12.179(2)	15.383(5)	10.104(2)	10.1279(5)	11.290(5)	10.9188(10)
c/Å	15.130(2)	18.694(3)	20.260(3)	19.603(3)	18.616(5)	21.9751(10)	18.8286(11)	20.312(5)	11.4628(10)
α/°	90	90	97.70(2)	91.63(2)	90	90	90	75.56(3)	90
β/°	107.159(10)	92.61(3)	91.46(2)	90.43(2)	92.61(2)	92.350(10)	91.568(3)	81.93(3)	112.876(2)
γ/°	90	90	92.32(3)	114.00(1)	90	90	90	62.24(4)	90
V/Å^3	2425.1(4)	3144.4(11)	2310.2(10)	2240.5(7)	3145(2)	3431.9(7)	3552.1(3)	1997.1(12)	1256.8(2)
Z	4	4	2	2	4	4	4	2	2
T/K	150(2)	150(2)	150(2)	150(2)	150(2)	150(2)	100(2)	150(2)	293(2)
μ(Mo-K$_\alpha$)/cm^{-1}	20.05	25.99	12.18	13.12	26.64	52.44	48.85	24.31	26.90
Reflections collected	4732	6207	8534	8349	5835	7571	27862	7621	5613
Unique reflections (R_{int})	4362 (0.0594)	5649 (0.0593)	8260 (0.0566)	7880 (0.0652)	5647 (0.0973)	6936 (0.1142)	8093 (0.0941)	7185 (0.0568)	1811 (0.0533)
*R*1 ($I > 2\sigma(I)$)	0.0426	0.0482	0.0578	0.0618	0.0908	0.0318	0.0481	0.0475	0.0312
w*R*′2 (all data)	0.1033	0.1398	0.1642	0.1932	0.2981	0.0785	0.0771	0.1407	0.0776

***trans*-[PtCl(PEt$_3$)$_2${Sb[C(O)(C$_6$H$_2$Me$_3$-2,4,6)]$_2$}] 20.** A solution of **18** (0.35 g, 0.74 mmol) in DME (10 ml) was added dropwise to a suspension of *cis*-[PtCl$_2$(PEt$_3$)$_2$] (0.19 g, 0.37 mmol) in DME (10 ml) at −78 °C. The resulting solution was allowed to warm to room temperature and stirred for 18 h. Volatiles were removed *in vacuo* leaving a red oily residue which was washed with hexane (40 ml) and extracted with diethyl ether (*ca.* 5 ml), filtered and the filtrate placed at −30 °C yielding **20** as red needles (yield 0.08 g, 22%), mp 115 °C (decomp.); NMR: ^{1}H (250 MHz, C$_6$D$_6$), δ 1.00 (dt, 18H, $^3J_{PH}$ 16, $^3J_{HH}$ 7.2, P(CH$_2$C*H*$_3$)$_3$), 1.96 (dq, 12H, $^2J_{PH}$ 22, $^3J_{HH}$ 7.2 Hz, P(C*H*$_2$CH$_3$)$_3$), 2.06 (s, 6H, *p*-ArCH$_3$), 2.50 (s, 12H, *o*-ArCH$_3$), 6.60 (s, 4H ArH); ^{13}C (100.6 MHz, C$_6$D$_6$), δ 7.24 (br s, P(CH$_2$*C*H$_3$)$_3$), 8.23 (br s, P(*C*H$_2$CH$_3$)$_3$), 18.63, 19.62 (s, ArCH$_3$), 127.9, 128.2 (ArCH), 131.2, 136.7, 145.8 (quat. ArC), 229.7 (SbC); ^{31}P{^{1}H} (101.2 MHz, C$_6$D$_6$) δ 14.5 (s, $^1J_{PtP}$ 3269 Hz, PEt$_3$); IR (Nujol, ν/cm^{-1}) SbCO 1664 s, 1603 s; MS APCI: *m*/*z* 148 (CH$_2$Me$_3^+$, 48%), 118 (PEt$_3^+$, 100%).

[Zn{As[C(O)Bu^t]$_2$[LiCl(DME)]}$_2$] 22. A solution of **10** (0.34 g, 1.14 mmol) in DME (20 ml) was added dropwise to a suspension of ZnCl$_2$ (0.08 g, 0.57 mmol) in DME (10 ml) at −78 °C. The resulting pale yellow solution was allowed to warm to room temperature and stirred for 24 h. Volatiles were removed *in vacuo* leaving a yellow oil which was washed with hexane (30 ml), extracted with diethyl ether (50 ml), filtered and the filtrate placed at −30 °C yielding **22** as pale yellow crystals (yield 0.13 g, 28%), mp 85 °C (decomp.); NMR: ^{1}H (400 MHz, C$_6$D$_6$), δ 1.80 (s, 36H, Bu^t), 3.42 (s, 8H, OCH$_2$), 3.65 (s, 12H, OMe); ^{13}C NMR (101.6 MHz, C$_6$D$_6$), δ 27.6 (C(*C*H$_3$)$_3$), 51.4 (*C*Me$_3$), 59.6 (OMe), 71.0 (OCH$_2$), 250.8 (AsC); IR (Nujol, ν/cm^{-1}) SbCO 1644 s, 1608 s; MS APCI: *m*/*z* 641 (M$^+$ − 2 DME, 79%), 245 (As{C(O)Bu^t}$_2$ 100%); calc. for C$_{28}$H$_{56}$O$_8$Cl$_2$-Li$_2$As$_2$Zn: C 40.9, H 6.8, found: C 39.69, H 6.79%.

[As{C(O)Ph}$_2$]$_2$ 24. A solution of **23** (0.42 g, 1.5 mmol) in DME (20 ml) was added to a solution of [Hg{N(SiMe$_3$)$_2$}$_2$] (0.3 g, 0.75 mmol) in DME (20 ml) at −50 °C. The resulting solution was allowed to stir for 4 h whilst warming to room temperature during which time deposition of mercury metal was observed. Volatiles were removed *in vacuo* and the green residue was extracted with hexane, filtered and concentrated to *ca.* 5 ml. Slow cooling of this solution to −30 °C afforded **24** as thin yellow plates (yield 0.12 g, 29%), mp 121 °C (decomp.); NMR: ^{1}H (400 MHz, C$_6$D$_6$), δ 7.31–7.45 (br m, 20H, ArH); ^{13}C NMR (101.6 MHz, C$_6$D$_6$), δ 123.4, 128.9, 131.2 (ArCH), 147.4 (quat. Ar), 181.0 (AsC); IR (Nujol, ν/cm^{-1}) AsCO 1695 s, 1645 s; MS EI: *m*/*z* 179 (AsC(O)Ph$^+$, 75%), 105 (C(O)Ph$^+$, 100%).

Structure determinations

Crystals of **8**, **11**, **13**, **15**, **16**, **19**, **20** and **22** suitable for X-ray structure determination were mounted in silicone oil whilst a crystal of **24** was mounted in epoxy resin. Crystallographic measurements were made using an Enraf-Nonius CAD4 diffractometer for all compounds except **20**, the data for which were collected on a Nonius Kappa CCD diffractometer. The structures were solved by direct methods and refined on F^2 by full matrix least squares (SHELX-97)[16] using all unique data. All non-hydrogen atoms are anisotropic with H-atoms included in calculated positions (riding model). A molecule of diethyl ether is included in the crystal lattice of **13** and a molecule of toluene is included in the lattice of **19**. The data for compound **16** are weak and as a result the structure did not refine as well as is normally expected. However, the fact that it is isomorphous with compound **11** leaves no doubt about its gross molecular framework. Crystal data, details of data collections and refinements are given in Table 1. The molecular structures of the complexes are depicted in Fig. 1–9.

CCDC reference numbers 165257–165265.

See http://www.rsc.org/suppdata/dt/b1/b105010a/ for crystallographic data in CIF or other electronic format.

Acknowledgements

We gratefully acknowledge financial support from EPSRC (studentships for T. C. W and R. C. T).

References

1 K. B. Dillon, F. Mathey and J. F. Nixon, in *Phosphorus: The Carbon Copy*, Wiley, Chichester, 1998 and refs. therein.
2 (*a*) C. Jones, *Coord. Chem. Rev.*, 2001, **215**, 159; (*b*) L. Weber, *Chem. Ber.*, 1996, **129**, 367 and refs. therein.
3 (*a*) J. Durkin, D. E. Hibbs, P. B. Hitchcock, M. B. Hursthouse, C. Jones, J. Jones, K. M. A. Malik, J. F. Nixon and G. Parry, *J. Chem. Soc., Dalton Trans.*, 1996, 3277; (*b*) C. Jones, J. W. Steed and R. C. Thomas, *J. Chem. Soc., Dalton Trans.*, 1999, 1541.
4 (*a*) *The Chemistry of Metal CVD*, ed. T. T. Kodas and M. J. Hampden-Smith, VCH, Weinheim, 1994; (*b*) J. T. Spencer, *Prog. Inorg. Chem.*, 1994, 145 and refs. therein.
5 C. Jones, S. J. Black and J. W. Steed, *Organometallics*, 1998, **17**, 5924.
6 S. J. Black, D. E. Hibbs, M. B. Hursthouse, C. Jones and J. W. Steed, *Chem. Commun.*, 1998, 2199.
7 (*a*) L. Weber, C. A. Mast, M. H. Scheffer, H. Schumann, S. Uthmann, R. Boese, D. Bläser, H.-G. Stammler and A. Stammler, *Z. Anorg. Allg. Chem.*, 2000, **626**, 421; (*b*) L. Weber, G. Meine, R. Boese and D. Bungardt, *Z. Anorg. Allg. Chem.*, 1987, **549**, 73.
8 L. Weber, K. Reizig and R. Boese, *Organometallics*, 1985, **4**, 1890.
9 A. B. P. Lever, *Inorganic Electronic Spectroscopy*, 2nd edn., Elsevier, Amsterdam, 1984.
10 F. A. Allen, O. Kennard, D. G. Watson, L. Brammer, A. G. Orpen and R. Taylor, *J. Chem. Soc., Perkin Trans. 2*, 1987, S1.
11 L. Weber, G. Meine and R. Boese, *Angew. Chem., Int. Ed. Engl.*, 1986, **25**, 469.
12 Value determined from a search of the Cambridge Structural Database.
13 G. Becker, M. Schmidt and M. Westerhausen, *Z. Anorg. Allg. Chem.*, 1992, **607**, 101.
14 D. F. Evans, *J. Chem. Soc.*, 1959, 2003.
15 R. C. Thomas, Ph.D. Thesis, Cardiff University, 2001.
16 G. M. Sheldrick, SHELX-97, University of Göttingen, 1997.